THE UNIVERSITY *of* EDINBURGH

Edinburgh Research Explorer

Receding-Horizon OPF for Real-Time Active Management of Distribution Networks

Citation for published version:
Robertson, J, Harrison, G & Wallace, A 2018, 'Receding-Horizon OPF for Real-Time Active Management of Distribution Networks' IET Generation, Transmission & Distribution, vol 12, no. 9, pp. 2124 – 2131. DOI: 10.1049/iet-gtd.2016.1939

Digital Object Identifier (DOI):
10.1049/iet-gtd.2016.1939

Link:
Link to publication record in Edinburgh Research Explorer

Document Version:
Peer reviewed version

Published In:
IET Generation, Transmission & Distribution

Receding-Horizon OPF for Real-Time Management of Distribution Networks

James Robertson, Gareth Harrison, Robin Wallace

School of Engineering, University of Edinburgh, King's Buildings, Edinburgh, UK
J.Robertson@ed.ac.uk

Abstract: This paper presents a new formulation for real-time active network management (ANM) control of distribution networks to maximise energy yield from distributed generation (DG). Coordinated scheduling of renewable DG and distribution network control assets can limit DG curtailment and significantly increase energy yield and economic performance of DG in weak or congested networks. Optimal power flow (OPF) has been employed in the literature for this purpose. However, single time frame snapshot formulations are limited by their narrow interpretation of temporal constraints. Here a formulation is presented for a new receding-horizon (RH) OPF technique to better control real-time ANM in distribution networks with high levels of temporally and spatially variable renewable DG. It is shown to improve the coordination between time sequences of system dispatch and improve voltage performance.

1. Nomenclature

Indices and sets:

g	Distributed generator index
b	Bus index
l	Line and transformer index
x	Grid supply point (GSP) index
k	Current time index
j	Control cycle index

Decision Variables:

$V_{b,reg}(j)$	CVC voltage target
$P_g^{curt}(j)$	DG real power curtailment
$\phi_g(j)$	DG power factor angle

State Variables:

$V_b\ (j)$	Voltage magnitude
$\delta_b(j)$	Voltage angle
$(p,q)^l_{b_1b_2}(j)$	Active and reactive power flows
$(p,q)_x(j)$	GSP active/reactive power exchange

Parameters:

p_g	DG real power capacity
$d_b^{P,Q}$	Peak real and reactive power demands
$\omega_g(j)$	Generation normalised resource level
$\eta(j)$	Demand normalised loading level
$V_b^{-,+}$	Upper/lower voltage bounds
$V_{b,reg}^{-,+}$	Upper/lower OLTC voltage bounds
s_l	Thermal rating of lines and transformers
$(p,q)_x^+$	GSP exchange limit
t_0	Control cycle timing reference
δt	Measurement delay time
Δt	Implementation delay time

2. Introduction

Distribution networks are undergoing an unprecedented period of change. Increasing levels of renewable distributed generation (DG) [1], evolution to a distribution system operator (DSO) [2], as well as new technologies, such as electric vehicles [3], are increasing operational complexity and creating planning challenges.

Active network management (ANM) [4] is expected to be deployed to handle future operation. Several projects have pursued ANM and flexible connection contracts in order to access 'spare' distribution network capacity. These have involved use of DG curtailment, thermal constraint management [5], voltage control [6]-[8], dynamic line ratings [9] and demand side management [10]. Each scheme takes on either a 'decentralised' or a 'centralised' form. The control actions or dispatch of decentralised schemes is determined based on local measurements and intelligence. Centralised ANM typically see the DNO using data measurement (or state estimation) to determine the network power flow conditions in real-time across a wider network area, and defining set-points for network and third party assets (including DG) to maintain safe operation. In line with the unbundled regulatory environment, the dispatch is 'technical' rather than 'economic' in nature.

Embedding localised control practices in distribution networks with bi-directional power flows has the potential to create operational conflict between new control practices, as well as established means. For example, simultaneous switching of voltage regulators can lead to over-correction, or step voltage violations. Non-simultaneous switching may incur a coarse form of hunting between control actuators. To avoid this [11] proposes a hierarchal approach for voltage control, using a decentralised scheme with temporal grading to prioritise local DG control practices over OLTCs. [12] presents a centralised logic based priority scheme for voltage control between DGs based on sensitivity and electrical distance.

The first generation of ANM controllers determined control set-points based on the assumption that measured power flow conditions will persist to the next control cycle. 'Persistence forecasting' can be susceptible to short-lived fluctuations in network conditions and fails to take into account how new control actions will impact the power flow regime in the next control cycle. Receding-horizon (RH) approaches offer a potential solution and have been used in optimisation strategies in real-time control environments [13]. The RH approach determines a rolling sequence of system set-points over an upcoming time period (control horizon), which are re-evaluated at defined intervening stages (control cycles) using updated system and forecast data. As such, they are better able to handle active control strategies, determining set-points that meet instantaneous and evolving system needs.

RH control has therefore been applied in power systems applications. [14] proposes a multi-agent RH control framework for local area voltage control in a transmission network in response to emerging voltage instability events; at each control cycle agents update and improve their response via neighbour-to-neighbour communication. [15] uses a multi-period optimal power flow (OPF) with a RH to schedule voltage controllers and restore nonviable or unstable transmission voltages to a “target-state”. [16] uses RH to prevent violation of ramp rate constraints between discrete runs of a multi-period, finite-horizon economic dispatch of generation. [17] uses a rolling multi-period optimisation to manage voltages and overloading by scheduling electric vehicle charging in (radial) LV networks. The results of RH algorithms depend on, and are sensitive to, the formation of the system forecasts. [16] and [17] utilise random number generators to disturb the time-series of power demands but assume a perfect forecast over the initial control interval. [18] developed a risk-based ANM approach to cater for wind power uncertainty: the risk level was based on output variance as determined from statistical analysis of historical data. This was used to inform the decision making in an optimisation based network management system and was shown to reduce the frequency and severity of network thermal and voltage violations. [19] used deterministic and stochastic RH controllers to dispatch energy storage in LV networks; the formulation involves demand forecasts generated by a scenario tree derived from a priori demand knowledge. [20] and [21] use an OPF and a two-stage relaxation process to optimise hourly day-ahead economic dispatch of a radial distribution system with renewables and energy storage; [21] demonstrates this on a real-time digital simulator. [22] uses a RH OPF for day-ahead hourly scheduling of energy storage with forecast variable generation; it uses a separate power systems estimator to ‘close’ the control loop at an hourly operational time step.

The authors’ earlier work [23] employed five-minute time-sequential OPF to actively dispatch a distribution network. This employed a pseudo ‘real-time’ network simulator [24] which mimics the rolling operation of a real system on a short time step (5 seconds). The separation of dispatch decisions and their implementation allowed a more realistic view of performance as the operation of individual controls is explicitly captured (e.g. transformer tap delay, voltage deadbands). The approach reduced the frequency and magnitude of voltage and thermal violations whilst minimising DG curtailment. However, the use of fast cycles of measurement and dispatch; and limitations with the use of persistence forecasting for near-term estimation of generation and demand suggested alternative approaches may provide value.

With this in mind, and building on an early outline of the idea [25], this paper substantially extends [23] to provide a new framework for receding-horizon control for centralised and coordinated ANM. The approach uses a rolling cycle of 30-minute generation and demand forecasts to produce a series of dynamic horizon forecasts from which network control set points are determined; these are simulated at a high time resolution in pseudo real-time. Furthermore, it incorporates a new time-indexed constraint within the OPF to minimise unnecessary changes in reactive power controls; this desensitises the system to large step changes in voltages. The application to multiple network constraints, data-streams and control time-frames, implemented on a coupled dispatch and real-time simulation architecture, makes the work unique in the literature.

This paper is structured as follows; Section 3 summarises the simulation environment and presents the formulation of the real-time receding-horizon OPF (RHOPF), detailing the forecasting application. Section 4 evaluates the RHOPF technique on a generic model of the UK medium voltage distribution network. Sections 5 and 6 discuss and draw conclusions.

3. Problem Formulation

3.1. Framework for Real-Time Simulation

A framework performing time-sequential power flow analysis simulating ‘real-time’ network operation across successive steady state intervals was presented in [25], [24]. The framework, shown in Fig. 1 (a), has two interfaced elements: (i) a distribution management system (DMS) within which a range of network management approaches can be articulated; and, (ii) a distribution network simulator (DNS) that translates commands within specific infrastructure in the ‘proxy’ distribution network. A dedicated distribution dispatch system (DDS) forms part of the distribution management system and is capable of hosting bespoke dispatch algorithms such as OPF or other formulations.

This system provides the opportunity to program and interpret new formulations for active management without acting directly on the control settings in the power flow. In addition, it allows the active regulation of individual DG and network asset controllers to be modelled explicitly in the power flow solution so that the control interactions and network response under ANM strategies can be observed.
Variable power flow conditions are modelled by time series profiles of generation and demand. The time series input data are fed exclusively to the power flow solutions of the ‘proxy’ distribution network. Sampling of ‘real time’ load and generation values, as well as prevailing network conditions, is carried out by the distribution management system and input into the dispatch system. This mimics operation of a realistic system. Here, the approach has been updated to facilitate the input and management of forecast data in the new RH formulation.

The OPF is formulated in the AIMMS optimisation modelling environment using the CONOPT 3.14A nonlinear solver. Plug-and-play of the OPF into the software environment via the COM interface allows the OPF to be implemented online. OpenDSS is the power flow engine used to simulate the ‘proxy’ distribution network.

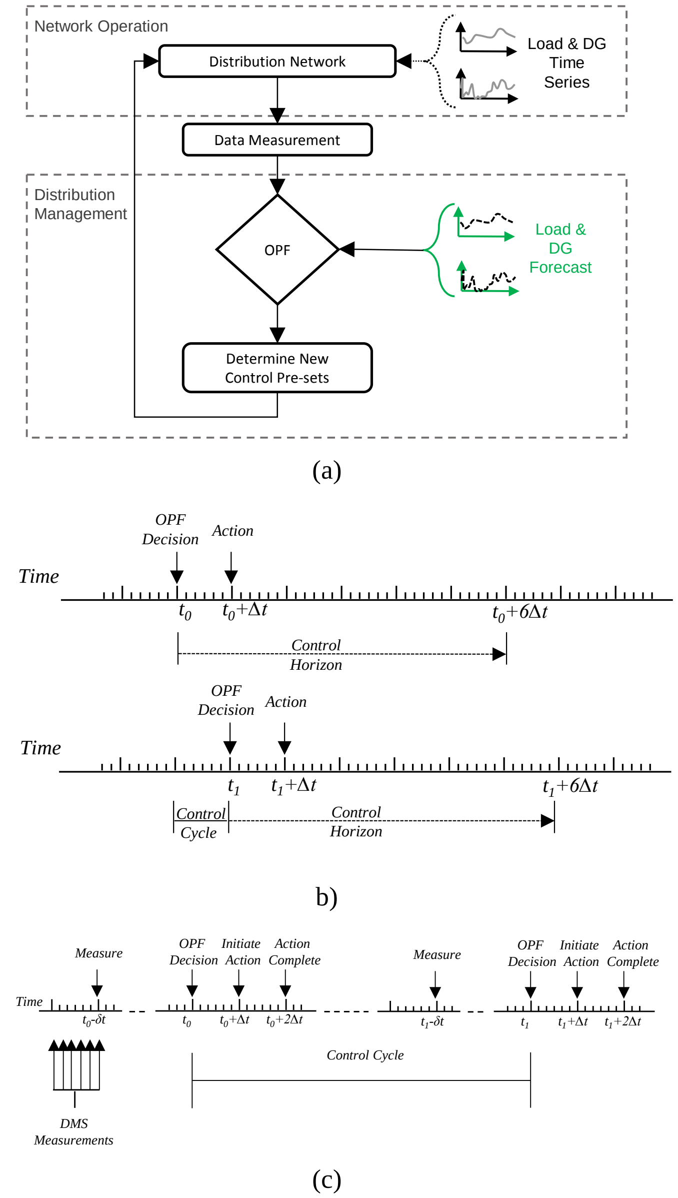

Fig. 1 *(a) Simulation Architecture; (b) Receding-Horizon Application and Control Interval; (c) Control Interval and DG Control Practice*

3.2. Receding-Horizon Formulation

The control scheme works as a time sequential feedback loop. For each time step the control scheme will:

1. Measure the prevailing network conditions and gather 'forecast' data;
2. Using a multi-period AC OPF determine a sequence of upcoming control set-points to manage voltage and thermal constraints within system boundaries;
3. Pass these new system control set-points to be implemented for the first control cycle.

The receding-horizon application is the continual automation of this process, as illustrated in Fig. 1(b). In this manner, the control horizon is continually receding and the network set-points are actively tracking optimal network configuration.

The methodology is applicable to a timescale best chosen to suit the unique circumstances of its application. The 'proxy' distribution network is simulated using steady-state power flow at 5-s time intervals, sufficient to show the network response to the implementation of new network control settings. The RH formulation operates on two distinct time intervals of network management, in the form of a control horizon, and control cycles. Here, the time horizon is 30-minutes within which there are a series of six sequential, 5-minute control cycles, as shown in Fig. 1 (b). Further information on the cycles is presented below.

<u>Control Cycle</u>

Within each control cycle a sequence of events simulates the real-time operation and network actions. These are illustrated in Fig. 1 (c) with the timing of actions expressed relative to the availability of new set-points from the dispatch algorithm, t_0. Communication, analysis and implementation time delays are illustrative but representative of real settings. The sequence of events is as follows:

'Measurement', time $t_0 - \delta t$: Measurements include the network state, prevailing resource availability and demand level. The delay, δt, is assumed to be 90-s.

'Dispatch', time t_0: Measurements are input to the DDS which produces new network and DG operating set-points for each of six consecutive 5-minute control cycles. Execution time is short compared to operational timescales.

'Instruction', time $t_0 + \Delta t$: The set-points are passed by the DMS to the 'proxy' network for implementation. The communications delay, Δ*t*, is assumed to be 30-s. The DDS prescribes individual target set-points for local control assets; these then invoke changes in local infrastructure as opposed to enacting direct control of local controllers.

'Completion', time, $t_0 + 2\Delta t$: Once the transition from the existing state is initiated, the control actions of each network component vary according to their own control practices. All actions are complete by this time. For DG active power output, the ramp to newly prescribed control setting occurs linearly across the interval Δ*t*. Changes to DG reactive power dispatch occurs in tandem with the active power dispatch. Should the voltage set-point require it, tap-changing transformers (OLTCs) follow standard operating practice with a (typical) 30-s delay prior to the tapping action.

<u>Control Horizon</u>

Each control horizon is a multi-period sequence of control cycles. In each instance, the operating set-points for each control cycle are determined by a RH 'forecast', which is created by linear interpolation between two sets of data: (i) 'real-time' network measurement as per the periodic control cycle and (ii) forecast data. For the purpose of illustrating the RH approach an (imperfect) 'forecast' is synthesised. This uses a central moving average smoothing process using a 15-minute interval of the real-time data for each generation resource and demand levels. A sample of the 'forecast' and the data on which it is based is illustrated for wind in Fig. 2. The RH forecast, that is the projected temporal variation for each DG resource and demand in each successive control horizon, is a linear interpolation from the measured prevailing resource level to the forward 15-minute and 30-minute forecast level. This process moves on with every 5-minute control cycle as illustrated in Fig. 3. Therefore, in each successive control horizon the point forecast value for

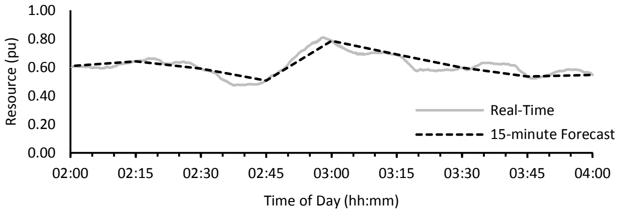

***Fig.* 2** *Illustration of wind power forecast data*

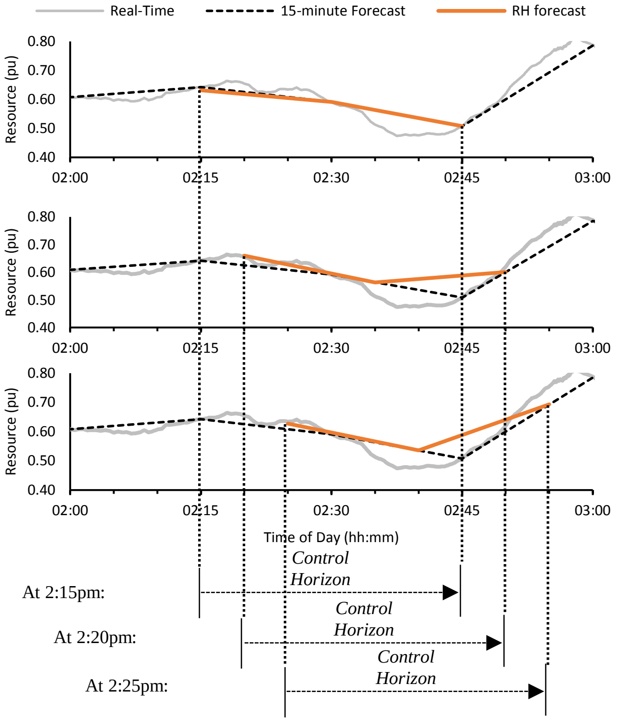

***Fig.* 3** *Illustration of the RH forecasting for wind*

the first control cycle, from which new network control set-points will be actioned, is close to the persistence value but transitioning towards the expected future conditions.

3.3. Distribution Dispatch: RH OPF Formulation

The dispatch of the network and DG set-points is carried out by a bespoke Receding Horizon OPF formulation. This is based on an earlier AC OPF [24] that has been substantially altered to handle multiple consecutive time frames and time-dependent control limits. It is designed to operate on a rolling basis, using a combination of data on generation output and demand loading levels 'sampled' from the network, and suitably generated forecast data.

In the RH approach, the time series of network power flows are evaluated consecutively over a control horizon composed of *j* discrete control cycles leading from the current time *k*. The algorithm returns projected solutions for each control cycle, subject to initial network conditions *k* ($k + j|k$). Warm start conditions across the horizon for each successive RHOPF solution are inferred from the last converged solution.

As DNOs do not currently perform economic dispatch of DG within their networks, dispatch is purely technical. The objective function therefore maximises the DG energy yield over time by minimising the curtailment of DG active power over each horizon control cycle:

$$Min \sum_{g\in G} p_g^{curt}(k+j|k) \qquad (1)$$

where p_g^{curt} is the active power curtailment of DG *g* (set *G*). The objective is subject to the range of normal power flow constraints, further enhancements of ANM control variables and special temporal network dispatch conditions to reduce network 'nuisance' switching.

The standard equations of network power flow include: the active and reactive nodal power balance (2-3); voltage (4) and thermal loading constraints (5-6). For brevity, the control horizon index ($k + j|k$) has been reduced to (j).

$$\sum_{l\in L|\beta_b^{1,2}=b} p_b^l(j) + d_b^P\eta(j) = \sum_{g\in G|\beta_g=b}\left[p_g\omega_g(j) - p_g^{curt}(j)\right] + \sum_{x\in X|\beta_g=b} p_x(j) \qquad (2)$$

$$\sum_{(l\in L|\beta_b^{1,2}=b)} p_b^l(j) + d_b^Q\eta(j) = \sum_{(g\in G|\beta_g=b)}\left[p_g\omega_g(j) - p_g^{curt}(j)\right]\tan\left(\phi_g(j)\right) + \sum_{(x\in X|\beta_g=x)} p_x(j) \qquad (3)$$

$$V_b^- \le V_b(j) \le V_b^+, \forall b\in B \qquad (4)$$

$$(p_{b_1,b_2}^l(j))^2 + (q_{b_1,b_2}^l(j))^2 \le (s_l)^2, \forall l\in L \qquad (5)$$

$$\left.\begin{aligned} -p_x^+ &\le p_x(j) \le p_x^+ \\ -q_x^+ &\le q_x(j) \le q_x^+ \end{aligned}\right\} \forall x\in X \qquad (6)$$

Here p_g is installed DG capacity; $d_b^{(P,Q)}$ denotes peak active and reactive demand at bus *b* (set *B*), $(p,q)_x$ are GSP flows, $(p,q)^l_{1,2}$ are the active and reactive power injections at the ends of each branch (denoted 1 and 2); and ϕ_g the DG power factor angle. Across each control horizon, $\omega_g(j)$ and $\eta(j)$ denote the per-unit resource and demand level, relative to installed capacity and peak load, respectively. The complex power injections at the ends of each branch are determined in terms of voltage magnitudes $V_b(j)$ and angles $\delta_b(j)$ by the standard Kirchhoff's voltage law formula. In the case of transformers, the primary voltage (V_i) must be divided by the transformer tap ratio, τ_l. For active management of the OLTCS and voltage regulators the tap ratio is constrained within the limits of each transformer:

$$\tau_l^- \le \tau_l(t) \le \tau_l^+ \qquad (7)$$

As small short term overloading of network assets was considered acceptable, power flow thresholds were set at rated capacity. However, a more conservative voltage envelope of ±5.5% nominal, rather than the regulatory ±6% was considered in the DMS formulation. This narrower range was employed to reduce the impact of real-time residual voltage variation within the proxy network due to, for example, the effect of discrete bandwidth on transformer taps.

ANM assumes that DNOs are capable of controlling existing network assets, such as tap changing transformers, and centrally dispatching DG active and reactive power output. Three control techniques are included in the OPF scheme: curtailment 8); variable Power Factor Control (PFC) (9-10) and Coordinated Voltage Control (CVC) (11).

$$0 \leq p_g^{curt}(j) \leq p_g \omega_g(j), \forall g \in G \tag{8}$$

$$\phi_g^- \leq \phi_g(j) \leq \phi_g^+, \forall g \in G \tag{9}$$

$$\left|\phi_g(j) - \phi_g(j-1)\right| \leq \Delta\phi_g, \forall g \in G \tag{10}$$

$$V_{b,reg}^- \leq V_{b,reg}(j) \leq V_{b,reg}^+ \tag{11}$$

Power curtailment is modelled as a simple reduction of production. The set-point issued to DGs is a per-unit reduction of the maximum resource-dependent power output and is therefore proportional to the forecasted resource levels, not DG capacity. This has the disadvantage of making it slightly more susceptible to forecast errors.

All DG is assumed capable of providing variable PFC by actively adjusting the DG power factor angle to absorb or inject reactive power as necessary. To reduce the potential circulation of reactive power, generation and absorption of reactive power by the DG was restricted to 0.98 leading and lagging. This was adopted to reflect the pre-existing ratio of local loading patterns. Due to the complex and differentiated relationship between independent control variables, additional governance is required to avoid unnecessary systematic switching: an additional constraint (9) limits the shifting of power factor control between control cycles. PFC can still be utilised to its full extent but requires a prior commitment. This constraint reduces instantaneous voltage spikes caused by the time differences between actions of each control element.

CVC allows dynamic control of regulated voltage levels of tap-changing transformers; in the optimisation it is modelled by relaxing the limits of the voltage at transformer regulated buses (11).

4. Case Study

The case study demonstrates the operation and effectiveness of the receding-horizon formulation in the UK Generic Distribution System (GDS) EHV1 [27] network, shown in Fig. 4 (a). The system is a section of weakly meshed network of parallel feeders supplied by two 30-MVA 132/33-kV transformers. A subsea cable between buses 318 and 304 connects the “mainland” to an “island” section. Voltage levels in the network are maintained by the substation OLTC, a voltage regulator (VR) between buses 304 and 321 and OLTCs at the 33/11-kV distribution transformers. The network also contains a 15-MVA rated interconnector, which is treated as a PV bus with a target voltage of 1pu.

Six DG locations and two renewable energy technologies were considered. Three wind farm developments at buses 1105, 1106, and 1108 and three tidal generation sites are connected at buses 1113, 1114, and 1115. The maximum headroom for DG at these locations was evaluated for two connection strategies in [26], as Table I shows. Under a ‘fit-

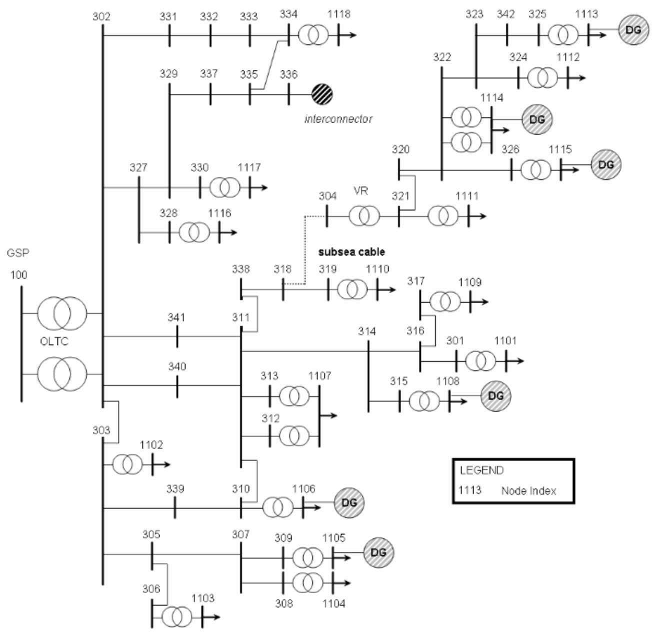

(a)

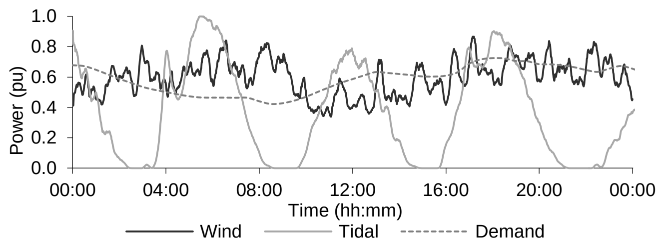

(b)

Fig. 4 *(a) UK GDS EHV1 network [26]; (b) 24-hour renewable energy resource generation and demand profiles (p.u. of nominal capacity and peak demand).*

and-forget’ philosophy, maximum DG capacity was limited to 20.5 MW, 55% of total system peak demand (38.2 MW); the binding constraint was voltage rise. With adoption of the ANM control strategies DG capacity increased to 52 MW; sections of the network consequently experience widespread reverse power flows and the active constraint on further DG capacity is a combination of voltage rise and the thermal limits on the 33/11-kV transformers, depending on the supply and demand conditions.

High resolution simulations were run for a 24-hour period. Fig. 4 (b) shows the demand pattern and generation profiles for wind and tidal generation. These are based on one second data from individual devices that have been aggregated and smoothed to reflect the pattern from medium sized farms. While the sequences of wind and tidal data are not concurrent their independence makes their use of value. The generation time series has been synchronised into 30-second intervals while the demand pattern was taken at 30-minute intervals. The data was synchronised to run concurrently and linearly interpolated between data points to very high resolution time steps in OpenDSS for use in the power flow simulations.

TABLE I

DG Installed Capacities

Location	Resource	'fit-and-forget' Capacity (MW)	ANM Capacity (MW)
1105	Wind	2.5	10
1106	Wind	10	15
1108	Wind	3	5
1113	Tidal	-	2
1114	Tidal	5	10
1115	Tidal	-	10
Total		20.5	52

TABLE II

Full EHV1 Results Summary

	'fit-and-forget'	Unconstrained	Snapshot OPF	RHOPF
DG Capacity (MW)	20.5	52	52	52
DG Production (MWh)	265.56	620.79	585.56	578.79
DG net Reactive Output (MVArh)	53.92	126.06	-24.75	-5.83
DG Energy Curtailed (MWh)	0.00	0.00	34.72	41.39
DG Energy Curtailed (%)	0.0%	0.0%	5.6%	6.7%
DG Capacity Factor	54.0%	49.7%	46.9%	46.4%
GSP (MWh)	-334.99	-25.59	-0.86	5.59
GSP (MVArh)	-182.93	-116.96	-210.83	-176.54
GSP power factor	0.878	0.214	0.004	-0.032
Network Losses (MWh)	14.3	29.2	24.4	20.0
Network Charge (MVArh)	22.1	52.7	47.9	41.5
Minimum Voltage	0.9760	0.9751	0.9547	0.9535
Maximum Voltage	1.0532	1.2445	1.0929	1.0809
Undervoltage Excursion*	0.00%	0.00%	0.00%	0.00%
Overvoltage Excursion*	0.00%	51.39%	5.56%	3.47%
Max. Thermal Loading (%)	75.14%	171.03%	130.96%	127.68%
Total overloading	0.0%	22.7%	10.1%	13.5%
Total Tap Changes	291	810	676	812

* Measured in 10-minute averages

To examine the value of the receding-horizon formulation, the analysis is compared with the 'fit-and-forget' connection capacity, unconstrained operation and dispatch using a sequential OPF operating at 5-minute intervals using a persistence forecasting routine, as in [24]. The latter two and the RHOPF employ the full 52 MW installed DG capacity. Reflecting standard UK practice the voltage levels in the 'proxy' distribution network results were assessed against the ±6% statutory limits, not the ±5.5% levels of the optimisation algorithms.

In keeping with earlier work a number of key metrics measure quality and effectiveness of the real-time controller: 1) volume of curtailment; 2) total voltage excursion measured as instantaneous peak and 10-minute averages to assess compliance with EN 50160 [28] (which permits short- term overvoltages <5% of time); 3) exceedance of branch flow limits measured as instantaneous peak relative to rated capacity and as percentage total instantaneous overload over the 24-hour test case; 4) frequency of OLTC taps; and 5) the reactive power demand at the Grid Supply Point (GSP, the transmission interface) which may indicate challenges for the transmission system to deliver this [29]. A summary of the simulation results are given in Table II.

1) Energy yield

Energy yield increases with the connected capacity and in comparison to the fit-and-forget case, energy yield in the ANM schemes was increased by 121% and 118% in the snapshot OPF and RHOPF respectively. Relative to the unconstrained case, both OPF and RHOPF mandate modest curtailment of available active power of 5.6% and 6.7%.

2) Voltage compliance

By definition, the fit-and-forget case experiences no voltage excursions but the unconstrained case sees frequent and extreme episodes. Both the snapshot and RHOPF ANM schemes vastly improved the voltage levels, bringing them predominantly within statutory and regulatory limits.

Observations of the voltage control measures indicated that the OPF and RHOPF formulations achieved voltage regulation via differing control means. In the snapshot OPF formulation, the optimisation favours voltage compliance primarily through the switching of the OLTC and VR tap-changing transformers, enforcing 'global' control strategies. In the RHOPF formulation, more localised control measures are deployed, with a preference for DG power-factor control and coordinated switching of local tap-changing transformers.

The differing preferences in the optimisation formulations have implications for the observed voltage compliance. The snapshot OPF formulation had a maximum instantaneous peak voltage level of 1.0929 pu and a total 10-minute average overvoltage excursion of 5.56%. The instantaneous peak is likely to cause tripping of overvoltage protection relays and the total overvoltage excursion does not comply with the 5% EN50160 limit. With the RHOPF formulation, the total overvoltage excursion was 3.47%, well below the EN50160 limit. Although lower than for the snapshot OPF, the maximum observed voltage level may still be problematic if sustained.

Sustained voltage excursion was almost exclusively concentrated on the primary winding of the 326-1115 transformer. Here the accumulation of residual overvoltage variation at high output from all island-connected DGs increases the voltage supply above statutory limits on the unregulated primary winding. This residual variation is dampened to the extent that voltage levels on the upstream VR transformer are within operational bandwidth resulting in no upstream voltage correction.

Analysing the network on a complex moving time-frame in the RHOPF case facilitated greater visibility of the fluctuating power flows caused by the renewable DG and significantly improves on the real-time performance of deterministic OPF snapshot solutions. Two examples of improved voltage compliance with the RHOPF case are illustrated in Fig. 5 to Fig. 7.

Fig. 5 shows the respective errors in the varying forecast strategies. Persistence forecasting for the snapshot OPF is inherently out of date by the point of implementation, while the RHOPF forecasting, with the look-ahead component, identifies the future ramping of DG and manages to evaluate and dispatch network set-points in-line or even in advance of changing power flow regimes Fig. 6 (top) shows the resulting dispatch of the generator real power set-point in each case.

The anticipation of further network constraints envisaged in the RHOPF means the generator active power set-point is not prematurely restored during a short dip in resource. In the snapshot alternative, the short-term evaluation resulted in a restoration of the active power set-point and a switch to alternative voltage control measures of generator reactive power and tap-changing transformers, which will be reversed in the near future. The consequences for real-time system voltage compliance are illustrated in Fig. 6 (bottom). Here, the snapshot OPF resulted in a sustained but minor system voltage excursion that is not evident for the RHOPF case where minimal re-configuration of settings was enacted.

A second example of improved voltage performance is illustrated in Fig. 7. Here, control delays between alternative voltage control measures are likely to induce short-lived voltage spikes which have the potential to trip protection relays. In the snapshot OPF case a large switch in power factor set-point at high power output caused the regulated voltage level to spike before corrective tap changing actions occur. With the RHOPF case, the rate of change for power factor control settings is constrained to mitigate high impact system control actions. This improves the steady state voltage profile, removes unnecessary control actions and reduces the overall number of system control switching.

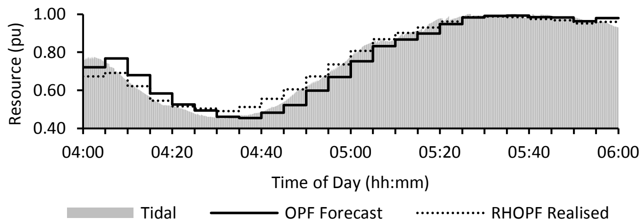

***Fig. 5** Time series trace of real-time tidal power forecast in the snapshot OPF and RHOPF*

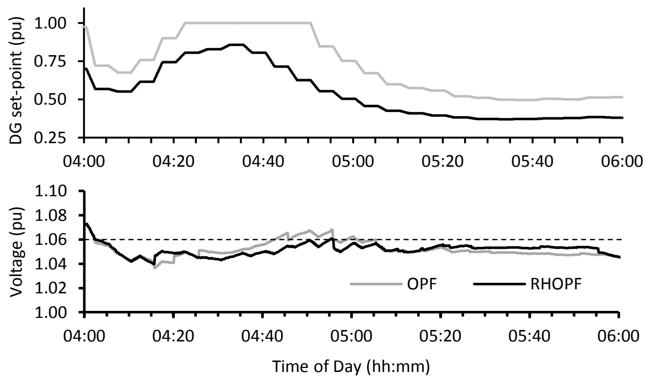

***Fig. 6** Time series traces of (top) tidal generator 1115 active power set-point and (bottom) Bus 326 voltage profile*

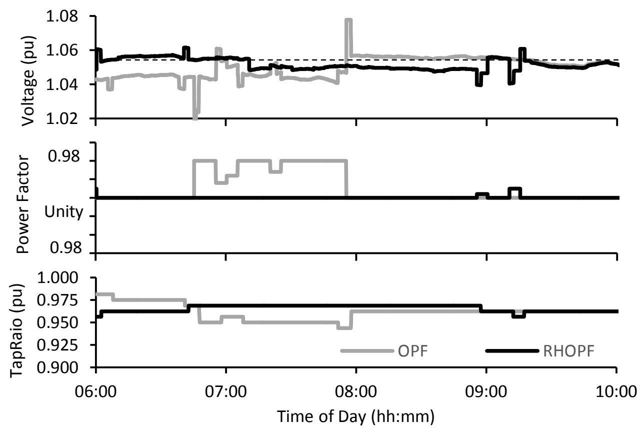

***Fig. 7** Time series traces of: (top) Bus 1106 voltage profile; (middle) WTG 1106 power factor set-point; and (bottom) bus 1106 distribution transformer tap positions.*

3) Thermal compliance

Short-term thermal overloading was considered acceptable and as such power flow thresholds of network plant were set at rated capacity. The unconstrained case experiences extensive and sustained overloading which the ANM schemes improve significantly. Some overloading persists in the optimisation cases as a result of forecast error.

Overloading of system components was restricted to the 33/11-kV distribution transformers upstream of the DGs. The maximum instantaneous thermal overloading observed was 131% of rated capacity for the snapshot OPF and 128% for the RHOPF. Over 10-minute averages these figures reduce to 113%. Total observed overloading was 10.1% in the snapshot OPF and 13.5% in the RHOPF. Total overloading was higher in the RHOPF case due to increased forecasting error. Relatively high values in each of these metrics might indicate that a change of strategy is required, however these values should be viewed in context with the high capacity factor of the test case. Further simulation is warranted to determine if this liberal approach to thermal compliance would be acceptable in practice.

4) Tap changing

The frequency of tap-changing actions varies in each case and the impact of ANM needs to be considered not only in overall terms but also on the type of transformer impacted: (i) the upstream OLTC and VR tap-changing transformers, and the local 33/11-kV distribution transformers (ii) with and (iii) without DG connected downstream.

Increased asset usage and increased variability means a significant increase in the number of tap-changing actions observed over the test case. Relative to the 'fit-and-forget' case the total number of tap-changing actions for all transformers increased for the snapshot OPF and RHOPF by 132% and 179%, respectively. Relative to the unconstrained case these have 15% and 20% fewer actions. The 20% higher tap changing actions in the RHOPF are the cost of improved voltage performance. Interestingly, this comprised a 9% reduction in upstream tapping actions, while actions were respectively 40% and 13.5% higher for the DG-connected and load only 33/11-kV distribution transformers.

ANM scheduling instigates significantly more local control switching. This differs from the conventional 'fit-and-forget' operational strategy, where the upstream voltage control actions maintain a global voltage profile, but reflects the greater levels of spatial variation to network power flows.

5) GSP reactive demand

The inclusion of DG power factor control as a means of mitigating voltage rise constraints means the impact on the network reactive power demand is significant and complex. The reactive power demand, show in Fig. 8 (middle) is sustained and uni-directional, with an average import of 8.8 MVAr and a spread of 4.7-16.3 MVAr. Taken in isolation this is not that significant, however, when viewed with respect to the network active power demand (Fig. 8 (top)), a bi-directional and quite complex withdrawal patterns from the upstream network exist. These range from 12.6 MW export to 11 MW import. This suggests that the challenging aspects of sustained reactive power demand is due to variation in active power import/export creating a constantly changing network power factor. Standard reactive power compensation may offer an easy and sustainable solution to this phenomenon.

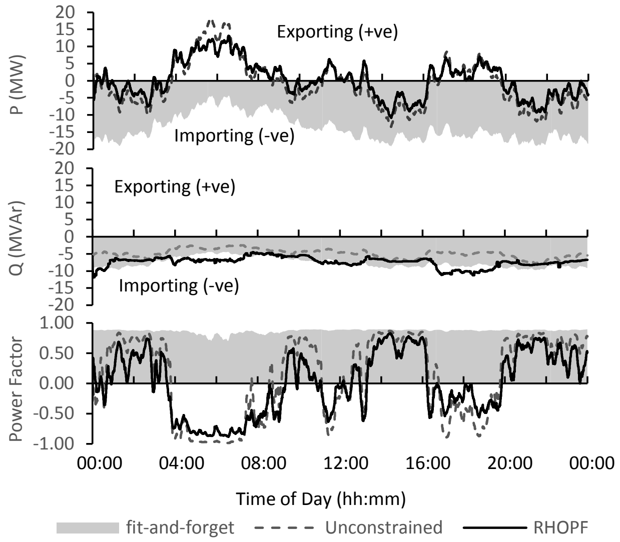

Fig. 8 *GSP power flow: (top) real; (middle) reactive; and, (bottom) power factor*

5. Discussion

Conventional distribution network control schemes rely on inflexible localised control practices, which adhere to conservative operational margins. These are often imposed by a lack of knowledge and vision of varying spatial and temporal network constraints. RH formulations are designed to implement optimisation strategies within the control loop (i.e. in real time), specifically to increase visibility of both these constraint types. Historically, RH dispatch and control schemes have been applied to slow-process systems. This work introduces the concept of RH-based optimisation to ANM control of distribution systems. It is envisaged that general future for DNOs in the UK will be to evolve into a DSO, where they will become increasingly responsible for actively managing the power flow and potentially, generation and consumption levels within their networks. This approach has many challenging technical, economic and regulatory aspects. These include the measurement and communication hardware requirements, associated data flows, data forecasting practices and amendments to distribution licencing.

The value of modelling using a real-time simulation framework is realised through analysis of the more realistic consequences of using integrated ANM techniques. This work has highlighted the potential for residual variations and short term spikes in system voltages as a result of control time delays which could invoke some unwarranted system disruption.

Additional governance was investigated to avoid unnecessary and harmful resolution of systematic switching from alternative control actions. Here an additional constraint on one control strategy reduces the impact of instantaneous voltage spikes caused by the time differences between the very fast-acting power factor control and delayed tap-changing actions. This phenomenon is likely to increase as further variables of active network management, such as demand side response, become available.

Beyond the impact of operational delays, it is not the purpose of this work to investigate the research and design of requisite measurement and communication technologies. As currently implemented, the optimisation formulation is fed ‘real-time’ information on all system generation and demand levels. The internal AC formulation of the optimisation power flow, is used to ‘fill in the blanks’ and determine the network state and control variable values. This significantly reduces the volume of associated data flows.

One significant requirement for the approach is the forecasting of power output from renewable energy resources and demand. In this analysis the RHOPF is fed streams of aggregated pre-processed data as a pseudo-forecast. However, one of the advantages of the RH approach, is that the horizon forecast does not have to be particularly accurate. While there is a significant advantage to accurate horizon forecasting, because the RH application will re-visit the control set-points at intermediate steps with a very short control cycle, the relatively long-term horizon forecast is never fully realised. The advantage of using a longer-term horizon forecast is to tune the temporal sequence of control set-points along the projected direction of optimal network configuration.

Finally, given the increasing levels of domestic solar PV generation currently connecting, one benefit and potential enhancement to the proposed approach that may be necessitated would be to consider net bus demand. This would require the demand forecast to capture the reduction of demand levels and in some cases negative bus demands. Using a combination of real-time network measurements and forecasting techniques, the receding-horizon application is particularly suited to the changing load composition.

6. Conclusion

This work demonstrated the use of a Receding-Horizon concept for real-time ANM control of DGs and active distribution network assets. Adoption of a centrally coordinated optimal control dispatch increased the network-wide energy yield. Results indicate that the RH formulation offers an improved voltage performance and significant improvements in the temporal stability of control settings, with a reduction in (global) control switching in favour of localised control actions to re-dispatch network settings. As a result the frequency and magnitude of network voltage excursions were reduced and were brought within regulatory limits. This indicates that the RH formulation offers one solution to the potentially harmful effects of short-term and even uncoordinated network switching. There remains an outstanding question over the ability to forecast intuitively, particularly for wind power generation, over the short control cycle control horizons. However, one specific advantage of the RH approach is that the furthest forecast prediction is never realised and serves only to generate possible optimal control trajectories from the current network state. Further enhancements, such as multi-objective and robust formulations of the optimisation technique, are warranted to investigate further applications of network directives and mitigate the concerns over network resilience to forecast errors.

7. Acknowledgments

This work is funded by the Engineering and Physical Research Council (grant numbers EP/F061242/1 and EP/I035773/1). The authors are grateful for valuable discussions with Dr Paul Trodden (Sheffield University).

8. References

[1] R.A.R. Walling, R. Saint, R.C. Dugan, J. Burke, & L.A. Kojovic, "Summary of Distributed Resources Impact on Power Delivery Systems," *IEEE Trans. Pwr. Dlvry*. 2008, *23, (3)*, pp. 1636–1644.

[2] Ofgem & Department of Energy and Climate Change - Smart Grid Forum, "Smart Grid Vision and Routemap," 2014. *Report Number: URN 14D / 056*, (February). http://doi.org/URN 14D / 056

[3] P. Papadopoulos, S. Skarvelis-Kazakos, I. Grau, L.M. Cipcigan, & N. Jenkins, "Electric vehicles' impact on British distribution networks," *IET Electrical Systems in Transportation*, 2012, *2*(3), pp. 91-102.

[4] DECC, Smarter Grids: The Opportunity, London, DECC, 2009.

[5] R.A. Currie, G.W. Ault, R.W. Fordyce, D.F. MacLeman, M. Smith, and J.R. McDonald, "Actively Managing Wind Farm Power Output," *IEEE Trans. Power Syst*., 2008, 23, pp. 1523-1524.

[6] M. Fila, D. Reid, P. Lang, J. Hiscock, and G. A. Taylor, "Flexible Voltage Control in Distribution Networks with Distributed Generation – Modelling Analysis and Field Trial Comparison," CIRED *20th International Conference on Electricity Distribution*, 2009, no. 0411.

[7] A. E. Kiprakis and A. R. Wallace, "Maximising Energy Capture from DGs in Weak Networks," *IEE Proc. Gen. Transm. Distrib*., 2004, 151, (5), pp. 611–618.

[8] T. Sansawatt, L. F. Ochoa, and G. P. Harrison, "Smart Decentralized Control of DG for Voltage and Thermal Constraint Management," *IEEE Trans. Pwr. Sys.*, 2012, 27, (3), pp. 1637–1645.

[9] T. Yip, G. Lloyd, M. Aten, B. Ferris, and C. An, Dynamic Line Rating Protection for Wind Farm Connections," CIRED 20th International Conference on Electricity Distribution, 2009.

[10] G. Strbac, Demand side management: Benefits and challenges. *Energy Policy*, 2008, *36*(12), pp. 4419–4426.

[11] Fallahzadeh-Abarghouei, H., Nayeripour, M., Hasanvand, S., & Waffenschmidt, E. (2016). Online hierarchical and distributed method for voltage control in distribution smart grids. IET Generation, Transmission & Distribution, 11(5), 1223-1232.

[12] Ranamuka, D., Agalgaonkar, A. P., & Muttaqi, K. M. (2016). Online coordinated voltage control in distribution systems subjected to structural changes and DG availability. IEEE Transactions on Smart Grid, 7(2), 580-591.

[13] J.M Maciejowski, "Predictive Control with Constraints," Prentice Hall, 2002.

[14] Islam, S. R., Muttaqi, K. M., & Sutanto, D. (2014). Multi-agent receding horizon control with neighbour-to-neighbour communication for prevention of voltage collapse in a multi-area power system. IET Generation, Transmission & Distribution, 8(9), 1604-1615.

[15] Glavic, M., Hajian, M., Rosehart, W., & Van Custem, T. "Receding-Horizon Multi-Step Optimization to Correct Nonviable or Unstable Transmission Voltages." *IEEE Transactions on Power Systems*, 2011, *26*(3), pp. 1641–1650.

[16] Xia, X., Zhang, J., & Elaiw, A. "An application of model predictive control to the dynamic economic dispatch of power generation." *Control Engineering Practice*, 2011, *19*(6), pp. 638–648.

[17] Connell, A. O., Flynn, D., & Keane, A. "Rolling Multi-Period Optimization to Control Electric Vehicle Charging in Distribution Networks." *IEEE Transactions on Power Systems*, 2014, *29*(1), pp. 340–348.

[18] Alnaser, S.W., & Ochoa, L.F. "Advanced Network Management Systems: A Risk-Based AC OPF Approach," *IEEE Transactions on Power Systems*, 2015, 30 (1), pp. 409-418.

[19] Rowe, M., Yunusov, T., Haben, S., Holderbaum, W., & Potter, B. "The real-time optimisation of DNO owned storage devices on the LV network for peak reduction." *Energies*, 2014, *7*(6), pp. 3537–3560.

[20] Moghadasi, S., & Kamalasadan, S. (2014, October). Real-time optimal scheduling of smart power distribution systems using integrated receding horizon control and convex conic programming. In Industry Applications Society Annual Meeting, 2014 IEEE (pp. 1-7). IEEE.

[21] Moghadasi, S., & Kamalasadan, S. (2016). Optimal fast control and scheduling of power distribution system using integrated receding horizon control and convex conic programming. IEEE Transactions on Industry Applications, 52(3), 2596-2606.

[22] Maffei, A., Srinivasan, S., Meola, D., Palmieri, G., Iannelli, L., Holhjem, Ø. H., ... & Glielmo, L. (2017). A Cyber-Physical Systems Approach for Implementing the Receding Horizon Optimal Power Flow in Smart Grids. IEEE Transactions on Sustainable Computing.

[23] J.G. Robertson, G.P. Harrison, & A.R Wallace, "OPF Techniques for Real-time Active Management of Distribution Networks," *IEEE Trans. Pwr. Sys.*, 2017, 32(5), pp. 3529-3537.

[24] J.G. Robertson, G.P. Harrison and A.R. Wallace, "A pseudo-real time Distribution Network Simulator for Analysis of Coordinated ANM Control Strategies", *CIRED Workshop: Integration of Renewables into the Distribution Grid*, Lisbon, Portugal, 29 May – 2 June 2012.

[25] Robertson, James, Gareth P. Harrison, and A. Robin Wallace. "A receding-horizon OPF for active network management." (2013): 1412-1412.

[26] L.F. Ochoa, C. J. Dent, and G. P. Harrison, Distributed Network Capacity Assessment: Variable DG and Active Networks, *IEEE Trans. Power Syst*., 2010, 25(1), pp. 87-95.

[27] Distributed Generation and Sustainable Electrical Energy Centre, United Kingdom Generic Distribution System (UK GDS). [Online]. Previously Available: http://www.sedg.ac.uk/.

[28] Power Quality Application Guide, 5.4.2 Voltage Disturbances Standard EN 50160: Voltage Characteristics in Public Distribution Systems, 2004.

[29] A. Keane, L.F. Ochoa, E. Vittal, C.J. Dent and G.P. Harrison, "Enhanced Utilization of Voltage Control Resources with Distributed Generation, "IEEE Trans. Pwr. Sys., 2011, 26(1), pp. 252-260.